A systematic error in MST/ST radar wind measurement induced by a finite range volume effect
2. Numerical considerations

Shoichiro Fukao

Radio Atmospheric Science Center, Kyoto University, Japan

Motoyuki Inaba and Iwane Kimura

Department of Electrical Engineering, Kyoto University, Japan

Peter T. May, Toru Sato, Toshitaka Tsuda, and Susumu Kato

Radio Atmospheric Science Center, Kyoto University, Japan

A finite range volume effect causes a systematic error in MST/ST radar wind measurement when a thin turbulent layer is simultaneously located in several adjacent range volumes. This error appears as a false vertical shear of horizontal wind or as a false temporal wind variation at some ranges even if the ambient wind field is uniform with height and does not change at all. Also, because of this effect the observed Doppler power spectrum becomes asymmetric, and a noticeable error is induced in estimation of echo power, mean Doppler velocity, and spectral width. The present investigation will show that these errors are well explained by a simple numerical model which is made to simulate an actual observational situation. The observed wind velocity is more reliable at ranges where the echo intensity is relatively larger compared with adjacent ranges. The finite range volume effect is negligibly small for weak ambient wind velocities less than approximately 10 ms^{-1} and/or for an antenna beam width less than one degree.

1. INTRODUCTION

The MST/ST radars employ three or more beam directions near the zenith which are not in a common plane to infer the wind vector [e.g., *Balsley and Gage*, 1980; *Röttger*, 1984]. If the radial velocities observed by the oblique beams are accompanied by a small amount of error, the horizontal wind estimation leads to a considerable error. One of the errors appears due to the finite range volume effect when a thin turbulent layer is simultaneously located in several adjacent range volumes [*Fukao et al.*, 1988] (hereafter referred to as paper 1).

As schematically shown in Figure 1, the wind velocity is observed to vary with height due to the finite range volume effect, even if the ambient wind field is uniform with height. The velocity is inferred to be larger at the upper range *A* and smaller at the lower

range *C* than the ambient wind velocity (which is correctly measured at *B*). This is because the zenith angle of the region from which the signal is effectively scattered back to the radar becomes larger at *A* than at *B*, while smaller at *C* than at *B*. Due to this effect, a positive vertical shear of horizontal wind is induced in a height range from *A* to *C*, even though the ambient wind field is uniform with height. The vertical scale of this false shear is a few hundred meters extended over several range volumes.

The false positive wind shears are generally accompanied by counter shears or negative shears since similar turbulent layers may exist above and/or below the layer considered (paper 1). Therefore an apparently wavelike oscillation with a small vertical scale is induced in height profiles of horizontal wind velocity as shown in Figure 15 of paper 1. This oscillation is false and needs to be discriminated from true wave oscillations.

Also, when the turbulent layer is displayed upward or downward within a range volume, the effect leads to a false temporal variation of wind, even if the
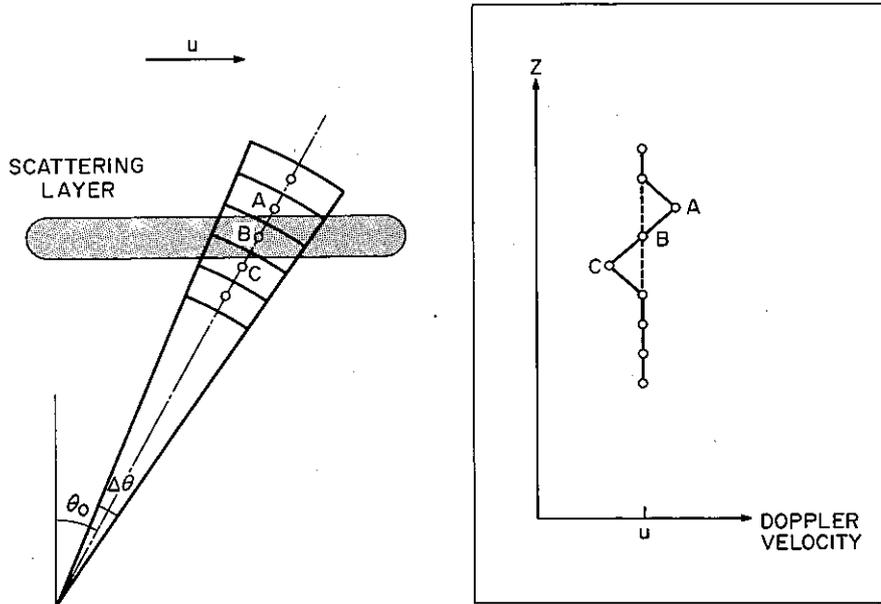
Fig. 1. A schematic diagram showing the finite range volume effect. (left) Vertical cross section of range volumes illuminated by the antenna beam of MST/ST radars (encircled by thick line). The beam is assumed to be tilted in a vertical plane parallel to the ambient horizontal wind u; θ_0 is the zenith angle of the apex (chain line) of the antenna beam with one-way half-power width of $\Delta\theta$. A thin horizontal turbulent layer indicated by shade is assumed to be simultaneously located at range volumes A, B, and C. (right) Height profile of horizontal wind velocity to be observed in the case shown on the left.

ambient wind field does not change at all. This velocity change appears only at a few ranges.

The finite range volume effect is discussed in paper 1 and *May et al.* [this issue], based on the observational data obtained by the MU radar of Japan [*Fukao et al.*, 1985a, b]. The finite range volume effect seems to occur quite frequently in the real atmosphere, but discrimination of true wind change from the false one is generally not easy in the observed data since the magnitude of the error depends on the unknown vertical distribution of turbulent layers (paper 1). Therefore, a quantitative discussion of this effect will be given in this paper based on a simple numerical model which is made to simulate the MST/ST radar observation. Distortion of Doppler power spectra due to this effect will be considered first, followed by estimation of the false radial shear of radial wind velocity.

A thin stratified turbulent layer located at h_c is assumed to have a backscatter cross section distribution which is uniform with respect to the horizontal direction, while the distribution is Gaussian with
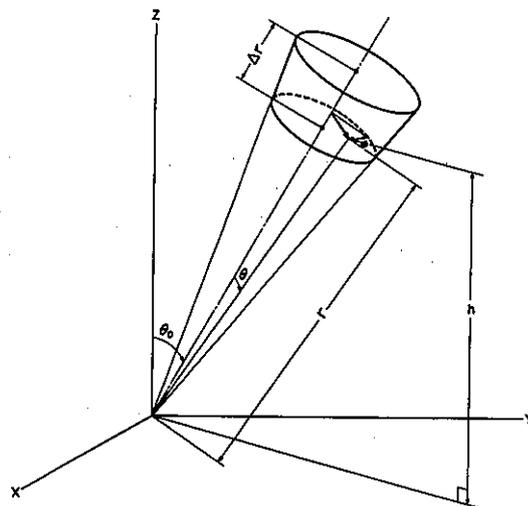

Fig. 2. Polar coordinate system used for the present numerical model; θ_0 is the zenith angle of the apex of the antenna beam shown by the chain line (assumed here to be tilted in the yz plane), while Δr is the range resolution. The ambient wind field u is assumed to be in the yz plane, and ϕ is the angle from the yz plane.

2. NUMERICAL MODEL

2.1. *Turbulent layer*

In the polar coordinates shown in Figure 2, height h is expressed as follows:

$$h = |r(-\tan\theta_0 \sin\theta \cos\phi + \cos\theta)| \cos\theta_0 \qquad (1)$$

half-power depth Δh in the vertical direction and has the form

$$I = I_0 \exp \left[-(h - h_c)^2/(\Delta h)^2/4 \ln 2\right] \tag{2}$$

where I_0 is the maximum backscatter cross section.

2.2. Antenna gain pattern

A one-dimensional antenna pattern with the same one-way half power beam width ($\Delta\theta$) of 3.7° as that of the MU radar antenna is considered. Irrespective of the beam zenith angles, its main lobe pattern is assumed to be as follows:

$$G = G_0 \left[\frac{\sin (\pi/\Theta)\theta}{(\pi/\Theta)\theta}\right]^{2.25} \tag{3}$$

where G_0 is the gain at the apex, and Θ is the angle to the first nulls (4.39°). It is shown in Figure 3 that the numerical model is a good approximation to the pattern along the north-south baseline of the MU radar antenna in the range within the first nulls [Fukao et al., 1985a]. Here, any contribution from side lobes, which has been extensively discussed by Watkins and Johnston [1985], is not taken into consideration.

2.3. Range weighting function

The range-weighting function is supposed to be a raised cosine function, as follows:

$$W = W_0 \left[\cos \frac{\pi}{\Delta r} (r - R_0) + 1\right]\bigg/2 \qquad |r - R_0| \le \Delta r$$

$$W = 0 \qquad\qquad\qquad\qquad |r - R_0| > \Delta r \tag{4}$$

where W_0 is the maximum receiver response, R_0 is the distance to the center of the range volume, and Δr is the range resolution.

2.4. Total Doppler power spectrum

The ambient wind field is assumed to be uniform, and no vertical wind is considered. Then, the radial velocity u_r, which is a projection of the ambient wind u to the beam direction (θ, ϕ), becomes

$$u_r = u(\sin \theta \cos \phi \cos \theta_0 + \cos \theta \sin \theta_0) \tag{5}$$

where the wind and beam are in the same plane. This assumption still gives a general result for observations of the mean Doppler shift, which is the main concern of the paper, but the spectral width and

shape will also be affected by wind component normal to the beam. However, it will be shown for this case that the finite range volume effect will have important effects on both the spectral shape and width.

Scattering from the turbulent layer is assumed to give a Doppler power spectrum of Gaussian shape with a half-power width of σ. The power spectrum has a mean Doppler shift v_D and is given by

$$P = P_0 \exp \left[-\frac{(u_r - v_D)^2}{(\sigma^2/4 \ln 2)}\right] \tag{6}$$

The above spectrum has a peak density of P_0 at $u_r = v_D$. Therefore the total Doppler power spectral shape observed by MST/ST radars $S(v_D)$ for a range R_0 is given by the following equation:

$$S(v_D) = \int_0^{2\pi} \int_0^{\Theta} \int_{R_0-\Delta r}^{R_0+\Delta r} IGWP \frac{\sin \theta}{r^2} dr \, d\theta \, d\phi \tag{7}$$

Note that for complete profiles, the profile will involve a convolution of the range weighting function and the backscatter cross section [Hocking, 1983, Hocking and Röttger, 1983]. This model assumes that the wind is in the same plane as radar beam and although the results concerning the mean Doppler shift will still be general, the spectral width will be affected by the transverse wind component [Hocking, 1983].
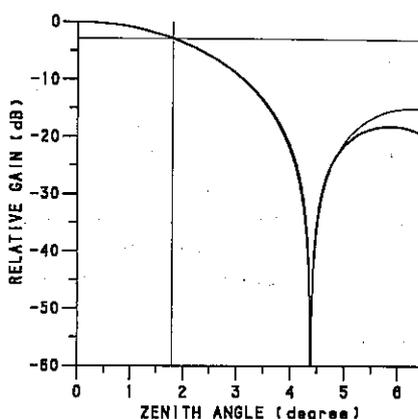
Fig. 3. One-dimensional antenna pattern used in the present numerical model. The pattern given by (3) is shown by thick line, while the pattern along the north-south baseline of the MU radar antenna is given by thin line. The first null points appear at a zenith angle of 4.39°.
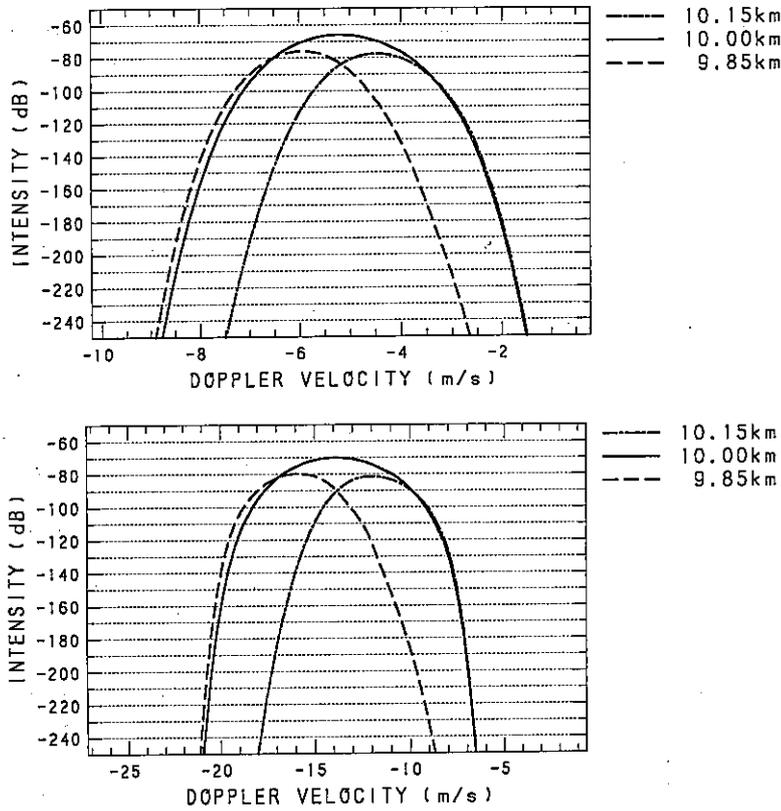
Fig. 4. Doppler power spectra calculated at three adjacent range volumes at heights of 10.15 (chain line), 10.00 (solid line), and 9.85 km (broken line), respectively. A turbulent layer with $\Delta h = 30$ m and $\sigma = 0.5$ ms^{-1} is supposed to be located at 10.0 km. The ambient wind velocities are (a) 30 ms^{-1} and (b) 80 ms^{-1}, respectively. Note that the abscissa scale of 4b is about 2 times larger than that of 4a.

3. RESULTS

3.1. Doppler power spectrum

Here it will be pointed out that a single thin turbulent layer may possibly affect the echo power, mean Doppler shift and spectral width observed not only at a single range but also at adjacent ranges. Generalized discussion based on the numerical simulation for a wide range of parameters is not the purpose of the present paper, and only the same situation as principally discussed in paper 1 is considered here: a turbulent layer is located in three consecutive range volumes as shown in Figure 1. A single turbulent layer with $\Delta h = 30$ m and $\sigma = 0.5$ ms^{-1} is supposed to be located at the center of the central range volume B at a height of 10.0 km. The beam direction (θ_0) is 10° from the zenith, while the range resolution (Δr) is 150 m.

Figure 4 shows Doppler power spectra calculated

at the three adjacent range volumes A, B and C, respectively (see Figure 1); 4a is for the horizontal velocity of 30 ms^{-1}, while 4b is for 80 ms^{-1}. Comparing the two results the spectral width becomes larger for larger horizontal velocity because of the finite beam width. It should be noted that only the spectrum calculated at B reflects the true wind velocity. The spectra at A and C lead to erroneous velocities although the ambient wind field is uniform with height.

The spectral widths calculated at A and C are narrower than those at B. Also, the spectral shapes at other than the central range volume are not symmetric with respect to their mean Doppler velocities, but the shapes are enhanced on the side of the true velocity compared to the other side. The spectral distortion becomes smaller with increasing Δh, being negligibly small for layers with Δh larger than Δr.

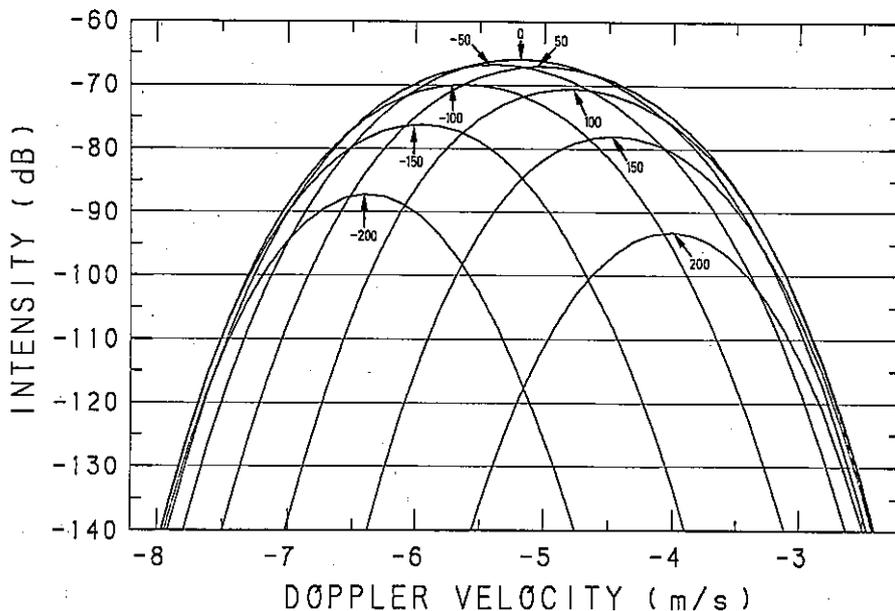The spectral shape also varies when the turbulent layer is shifted upward or downward. Figure 5 shows

Fig. 5. Doppler power spectra calculated for the case that the layer center is shifted upward (positive) or downward (negative) from the center of the range volume a distance ±50, ±100, ±150, and ±200 m, respectively. Other parameters except for $u = 30$ ms^{-1} are the same as those in Figure 4.

the spectra calculated for the central range volume when a turbulent layer with the same parameters as above is shifted upward or downward a distance of 50, 100, 150, and 200 m, respectively. The horizontal velocity is assumed to be 30 ms^{-1}. The inferred (radial) velocity differs by nearly 2.5 ms^{-1}, or about half of the true radial velocity of the ambient wind,

when the layer height changes by ±200 m, an equivalent effect to that observed by Hocking [1983]. This difference is proportional to the ambient wind velocity.

A change of antenna beam direction also leads to different spectral shapes. Figure 6 shows the spectral shapes calculated for the cases that the beam is
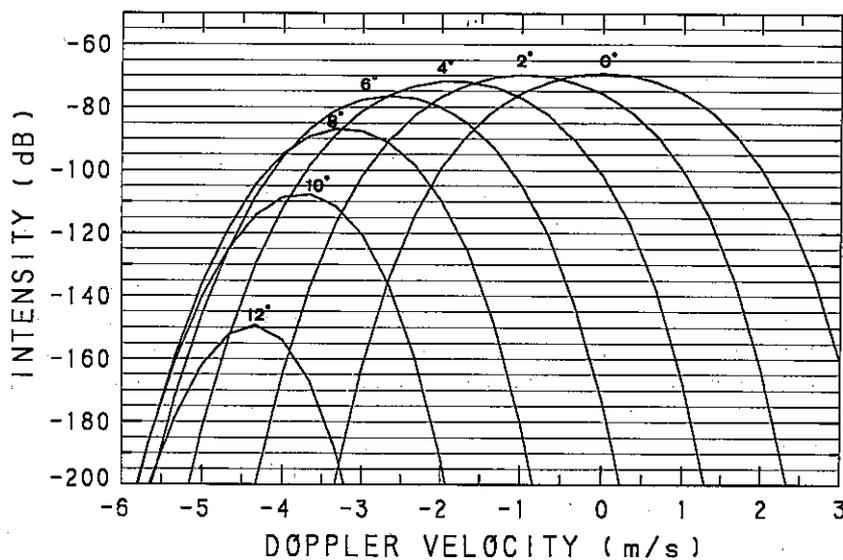

Fig. 6. Doppler power spectra for the beams directed to seven different directions with angles of 0, 2, 4, $\cdots$, 12° from the zenith, respectively. Other parameters are the same as those in Figure 5.

31-DEC-1985 2207LT
- 1-JAN-1985 0036LT

(Az,Ze)-(90,15)
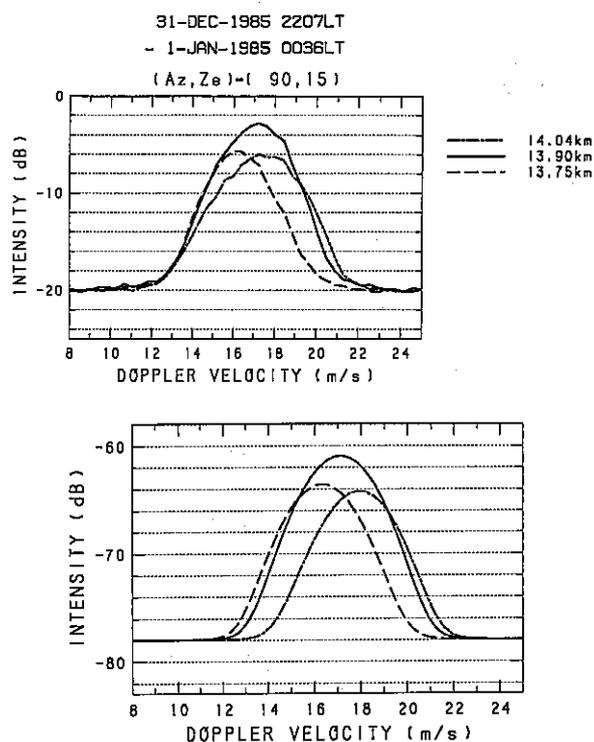

14.04km
13.90km
13.75km

Fig. 7. (a) Doppler power spectra observed by the MU radar in a 2.5-hour period from 2207 LT (LT is local time (Japan standard time)) on December 31, 1985 to 0036 LT on January 1, 1986. The beam direction is 15° eastward (90° azimuth from the north) from the zenith. The spectra at 14.04, 13.90, and 13.75 km are given by chain line, solid line, and broken line, respectively. (b) Theoretical Doppler power spectra that resemble the observed ones by choosing the parameters of the numerical model. The horizontal velocity is 66 ms^{-1}.

pointed to seven different directions, with separation of 2°, in the region from the zenith to the 12° off zenith. The turbulent layer is located at 75 m above the range center of the zenithal beam (i.e., 10.075 m in height). The spectral shape changes substantially with increasing zenith angles, especially, in the direction of 10° and 12° from the zenith. The spectral width becomes narrower as the beam is tilted more, since signal is received from a smaller range of angles. It is noted that the decrease of echo intensity with increasing beam zenith angle does not reflect the aspect sensitive scattering [e.g., Gage and Balsley, 1980], since the scattering is assumed to be isotropic in the present model. Also, the radial velocity estimate from the mean Doppler shift becomes more negative than the true projection of the horizontal wind when the beam is tilted more from the zenith. The finite range volume effect does not appear in the zenith direction. On the other hand, it is shown that

the mean Doppler shift changes very little when spectral width σ is varied.

The spectra observed by the MU radar at three adjacent heights near 14 km, where a typical false wind shear due to the finite range volume effect is found (paper 1), are given in Figure 7a. They are the average of the 2.5 hr period data shown in Figure 14 of paper 1. Figure 7b shows the theoretical spectra that resemble closely the observed ones shown in 7a. They are calculated by assuming a single turbulent layer with $\Delta h = 200$ m and $\sigma = 2.0$ ms^{-1} which is located 10 m below the center of the central range volume. The white noise is added so as to make the detectability of numerical spectra approximately equal to the observed ones. As shown in Figure 14a of paper 1, an intense turbulent layer was continuously observed at the same height during this period. This presumably supports the assumed spectral parameters which suit a fairly strong turbulent layer.

The above turbulence parameters are presumably not the optimum ones, but it is not considered as important to investigate parameters more suitable to the observed spectra. It will be only noted that the close resemblance between the observed and numerical spectra is consistently obtained at three different ranges by assuming the finite range volume effect for a single turbulent layer.

3.2. Shear-velocity ratio

In Figure 8 false radial shears of radial wind velocity Λ_r (radial-velocity shear) induced by the finite range volume effect are calculated. The numerical model is the same as that used in Figure 4 except for Δh and u. The calculation is performed for both $\Delta h = 60$ m and 30 m for u changing from 10 to 100 ms^{-1}.

As expected, Figure 8 illustrates that the radial-velocity shear Λ_r increases almost proportionally with u. When u is larger than approximately 50 ms^{-1}, Λ_r exceeds 1.04 ms^{-1}/ΔR, which corresponds to 40 ms^{-1} km^{-1} of a vertical shear in horizontal wind. Wind shears with magnitude larger than this value generate Kelvin-Helmholtz instability for the ordinary potential temperature gradient in the troposphere and stratosphere.

The gradient of the curve shown in Figure 8 gives the ratio of radial-velocity shear to radial velocity (Λ_r/u_r is shear-velocity ratio) (paper 1). Figure 9 shows the calculated shear-velocity ratio against different beam widths for $\Delta h = 60$ and 30 m. The diagram also includes the observational maximum values shown in Figure 9 of paper 1. The observed
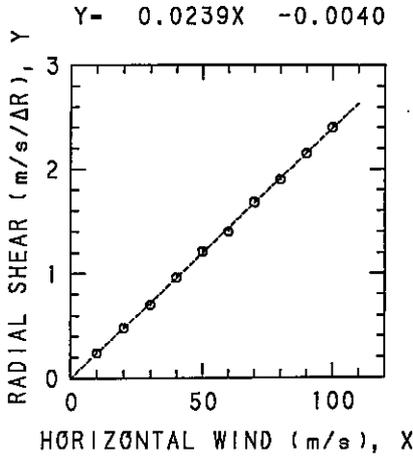
Y= 0.0239X -0.0040

Fig. 8. False radial-velocity shear $\Lambda_r(Y)$ induced due to the finite range volume effect versus horizontal wind velocity u (X). The beam width is assumed to be 3.7°. The ordinate is magnitude of the shear per unit range volume $(\Delta R = 150$ m$)$. The linear relationship between X and Y determined by a least mean square fitting is given by dotted line.

results are the average over a period of 16 hours. The general tendency of the observed results seems to be consistent with this simple theoretical model of the finite range volume effect.

By extrapolating the data in Figure 9 to narrower beam widths, it is found that the beam width should be smaller than 0.5° in order that the finite range volume effect is insignificant. Such a narrow beam will not be expected for ordinary MST/ST radar antennas, but a false vertical shear of the horizontal wind on the order of 1 ms^{-1} km^{-1} or $\Lambda_r \sim 0.03$ ms$^{-1}/\Delta R$ may be practically admitted. Thus from this diagram accurate wind estimations free from the finite range volume effect are expected to be made if the beam width is less than 1°.

In the case that the same turbulent layer exists simultaneously at two adjacent range volumes instead of three, the radial-velocity shear calculated for the same parameters leads to almost the same magnitude as that of the three-range-volume model. This is not always true, but the magnitude of the radial-velocity shear varies considerably depending on the beam zenith angle, beam width, and range resolution, as well as height and thickness of the turbulent layer as discussed in paper 1. Also, the magnitude of the shear is affected by the spectral distortion mentioned in section 3.1. The number of range volumes in which the turbulent layer is simultaneously located is another factor to determine the magnitude, with thicker turbulent layers allowing more range volumes. Thus

it is too complicated to discuss the finite range volume effect in a generalized way. We are inclined not to do so beyond noting that the three-range-volume model is one of the cases that may actually exist in the real atmosphere, considering a layer thickness of 100 m or less.

3.3. Effective beam width for scattering

If the scattering occurs primarily near the edge of the beam width, Λ_r/u_r becomes twice as large as the present numerical values (paper 1). This difference indicates that the dominant scattering occurs, on the average over a considerably long duration, from the inner region of the beam width, although sometimes the scattering may also occur at the edges of the beam. The effective scattering region, or equivalent half-power beam width $\Delta\theta_e$, is given by

$$\Delta\theta_e = \alpha\Delta\theta \qquad (8)$$

where $\alpha < 1$. The shear-velocity ratio per unit range volume is expressed as (paper 1)

$$\Lambda_r/u_r = \cot\theta \sin(\alpha\Delta\theta/2) \qquad (9)$$

where α is determined by fitting (9) to the numerical data shown in Figure 9 in a least mean square sense. The result is $\alpha = 0.675$. Thus the effective beam width is $\Delta\theta_e = 3.7° \times 0.675 = 2.49°$.

The above result suggests that the virtual beam

⊙ :60m thickness Y= 0.036X- 0.018
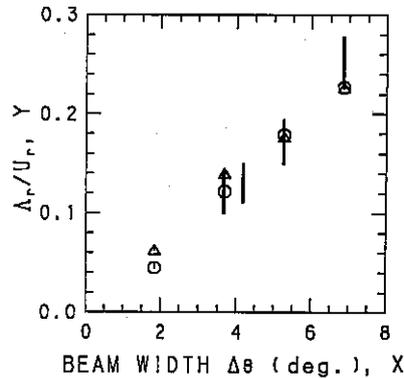△ :30m thickness Y= 0.032X+ 0.010
━ :observed

Fig. 9. False shear-velocity ratio Λ_r/u_r (Y) versus beam width $\Delta\theta$ (X). The ratio is given by the gradient of the curves of radial-velocity shear versus radial velocity for respective beam widths. The turbulent layer is assumed to be 60 or 30 m in thickness. The linear relationship between X and Y given for each layer thickness is determined by a least mean square fitting. The thick vertical bars indicate the observed values shown in Figure 9 of paper 1.

direction may occasionally deviate from the physically pointed direction by, at largest, $\Delta\theta_e/2 = 1.25°$ due to the finite range volume effect. This deviation will lead to a wind estimation error as

$$u_{err} = u \cot \theta \sin (\Delta\theta_e/2) \qquad (10)$$

For $\theta = 10°$ and $\Delta\theta = 3.7°$, $u_{err} = u \times 0.123$. This means that the error caused due to the finite range volume effect is, on the average, approximately 12% of the horizontal wind velocity. The error may sometimes be twice as large as the mean value of the error. This magnitude is by no means negligibly small, but it is not fatally large.

4. CONCLUSIONS

The finite range volume effect is investigated based on a numerical model that simulates the actual MST/ST radar observation. It is pointed out that if there exists a stratified turbulent layer thinner than the range resolution, the velocity estimation will give different values according to the height of the layer within the range volume, even if the ambient wind field is uniform with height. This may induce a false wind shear and/or a wind oscillation when the thin turbulent layer is simultaneously located in several adjacent range volumes. Their vertical scale is of the order of a few hundred meters. Even for moderate wind velocities the magnitude of the false shears may become larger than the critical value, above which the Kelvin-Helmholtz instability will be generated in the real wind shear.

Also, this effect leads to a wind estimation error of, on an average, more than 10% of the horizontal wind velocity, but sometimes there may be up to twice this error. Therefore discussion of the fine structure of the wind profiles obtained by MST/ST radars with antenna beam width of 3°–4° or larger should be performed carefully.

The present paper is limited only to the case of zenith angle of 10° and at a height of 10 km where the jet stream predominates. But the same calculations performed for other turbulence parameters lead to slightly different but essentially the same results.

Due to the finite range volume effect, a single turbulent layer may influence Doppler velocities estimated at three or four adjacent range volumes in the troposphere and stratosphere, and presumably at more ranges in the mesosphere where turbulent

layers are probably thicker and range resolutions used are generally much larger than in the troposphere and stratosphere. The greater the wind velocity, the larger the error becomes.

Considering the consequences of the finite range volume effect, the following cases can be regarded as true physical processes. First, features observed successively over more than seven or eight range volumes will be real. Second, the features observed for weak ambient wind velocity are real (paper 1). Third, the spectral shape as well as the vertical velocity obtained in the zenith direction does not suffer substantially from the finite range volume effect, although there is some dependence on spectral width with range [Hocking, 1983]. Fourth, the wind velocity is comparatively reliable at the ranges where the echo power is larger compared with those above and below the layer (paper 1). Since the turbulent layer is not necessarily located at the center of each range volume, the precise wind profile should be formed using only the reliable estimates at adjacent ranges. Finally, the Doppler power spectra will be correct when obtained by the beam less than 1° in width, for which the finite range volume effect is virtually negligible.

REFERENCES

Balsley, B. B., and K. S. Gage, The MST radar technique: Potential for middle atmospheric studies, *Pure Appl. Geophys.*, *118*, 452–493, 1980.

Fukao, S., T. Sato, T. Tsuda, S. Kato, K. Wakasugi, and T. Makihira, The MU radar with an active phased array system, 1, Antenna and power amplifiers, *Radio Sci.*, *20*, 1155–1168, 1985a.

Fukao, S., T. Tsuda, T. Sato, S. Kato, K. Wakasugi, and T. Makihira, The MU radar with an active phased array system, 2, In-house equipment, *Radio Sci.*, *20*, 1169–1176, 1985b.

Fukao, S., T. Sato, P. T. May, T. Tsuda, S. Kato, M. Inaba, and I. Kimura, A systematic error in MST/ST radar measurement induced by a finite range volume effect, 1, Observational results, *Radio Sci.*, this issue.

Gage, K. S., and B. B. Balsley, On the scattering mechanisms contributing to clear air radar echoes from the troposphere, stratosphere, and mesosphere, *Radio Sci.*, *15*, 243–257, 1980.

Hocking, W. K., On the extraction of atmospheric turbulence parameters from radar backscatter Doppler spectra, I, Theory, *J. Atmos. Terr. Phys.*, *45*, 89–102, 1983.

Hocking, W. K., and J. Röttger, Pulse length dependence of radar signal strengths for Fresnel backscatter, *Radio Sci., 18*, 1312–1324, 1983.

May, P. T., S. Fukao, T. Tsuda, T. Sato, and S. Kato, The effect of thin scattering layers on the determination of wind by the Doppler technique with MST radars, *Radio Sci.*, this issue.

Röttger, J., The MST radar technique, in *Handbook for MAP*, vol. 13, edited by R. A. Vincent, pp. 187–232, University of Illinois, Urbana, Ill., 1984.

Watkins, B. J., and P. E. Johnston, Antenna-induced range smearing in ST and MST radars, *Radio Sci., 20*, 1130–1140, 1985.

S. Fukao, S. Kato, P. T. May, T. Sato, and T. Tsuda, Radio Atmospheric Science Center, Kyoto University, Uji, Kyoto 611, Japan.

M. Inaba and I. Kimura, Department of Electrical Engineering, Kyoto University, Yoshida, Kyoto 606, Japan.